CSAWAC 47 (2) (2019) · Vol. 47 · No. 2 · February 2019

# CLEAN
## Soil Air Water

Renewables

Sustainability

Environmental Monitoring

2 | 2019

www.clean-journal.com

WILEY

# Abatement of Amoxicillin, Ampicillin, and Chloramphenicol From Aqueous Solutions Using Activated Carbon Prepared From Grape Slurry

*Rumbidzai Chitongo, Beatrice O. Opeolu, and Olatunde S. Olatunji**

**The adsorption of amoxicillin (AMX), ampicillin (AMP), and chloramphenicol (CHLR) from simulated antibiotic-contaminated water using adsorbents prepared from grape slurry waste is studied. Batch adsorption experiments are carried out to evaluate the adsorption capacity of the adsorbents for AMX, AMP, and CHLR. Adsorption isotherms are described by the Langmuir and Freundlich isotherms, while the pseudo-second order kinetics describe the sorption processes. Negative values of the enthalpy change show that the sorption processes are exothermic, and the positive values of the Gibbs free energy change indicates non-spontaneous but feasible nature of the adsorption. The study shows that grape slurry waste could be a good precursor to prepare effective adsorbents for the remediation of antibiotic-contaminated wastewater.**

## 1. Introduction

The therapeutic and prophylactic use of pharmaceutical compounds for the promotion of human and animal health has tremendously increased in recent times. Several classes of pharmaceutical compounds are known and administered for different types of diseases. Among the different pharmaceuticals are the antibiotics, one of the largest pharmaceutical classes of drugs applied for the treatment and prevention of bacteria and other microbial infections. Antibiotics are compounds of different sub-classes having precursor structures largely encompassed by cyclic components, represented by either benzene rings, piperazine units, hexahydropyrimidines, sulphonamides, quinolone, or morpholine groups.[1,2]

Pharmaceutical compounds including antibiotics are synthesized in such a way that they are bio-activity specific, resisting deactivation until their intended action is accomplished, that is, producing desired biological effects upon administration.[3–5] About 60–80% of orally administered doses may remain un-metabolized, and are excreted through sweat, urine, and feces.[3–6] They therefore reach water and other environmental compartments through releases from various sources including domestic, agricultural, and industrial discharges. Water is essential to sustain life, but its deterioration in quality and quantity is increasing pressure on water resources globally.

Most antibiotics possess unique characteristics such as polarity, polymorphism, complex chemical structures, ability to be ionized, and having multiple ionization sites on their molecules. These properties impact on the variable ability to resist degradation, hence they are "pseudo-persistent," and may persist long in different environmental matrices, resulting in their accumulation and/or redistribution.[7] Residues of some prescribed antibiotics have been detected at trace and ultra-trace concentrations in different aquatic environments worldwide.[8,9] This portends a problem because of their capacity to induce toxic consequences on unintended organisms that may be exposed to them. Antibiotic resistance, for instance, has been indicated for potential aquatic toxicity, genotoxicity, and endocrine disruption.[9,10–14] Chayid and Ahmed[15] also suggested that occurrence of antibiotics in aquatic environments may pose potential adverse effects, including acute and chronic toxicity on humans and animals via indirect contact or through heterotrophic translocations.[3,8,15]

The accumulation, environmental stability, and observed toxic effects of pharmaceutical compounds on unintended organisms have attracted interest in the scientific community. As a result, they have been listed among the contaminants of emerging environmental concern.[16–19]

Urban surface water, municipal sewer networks, and wastewater treatment plants (WWTPs) are likely hot spots of antibiotics to the environment.[20] Water and other compartments of the environment can be contaminated by the receipt of effluent discharges from households, pharmaceutical manufacturing plants, hospitals, direct discharge of untreated wastewater from leaking septic tanks, landfills leachates, direct disposal of therapeutic drugs, and the use of WWTP sludge as fertilizer in agricultural fields, etc.[5,9,10,21,22] Fecal matter contaminated with these compounds also reach surface water bodies through surface runoffs due to lack of proper sanitation.[5,23]

R. Chitongo, B. O. Opeolu
Faculty of Applied Sciences
Department of Chemistry
Cape Peninsula University of Technology
Cape Town, South Africa

O. S. Olatunji
School of Chemistry and Physics
College of Agriculture, Engineering and Science
University of KwaZulu-Natal
Durban 4000, South Africa
E-mail: snf_olatunji@ymail.com

**DOI: 10.1002/clen.201800077**

 

WWTPs are used for treatment of wastewater to ensure that it falls within the quality acceptable for discharge into the aquatic ecosystem, but they have failed to ensure safety of wastewater discharge.[9] Global scientific evidence have suggested that most WWTPs cannot completely remove micro-organic pollutants during treatment processes because they were not designed to eliminate micro-organic pollutants such as pharmaceuticals.[5,24–26]

High-cost techniques such as precipitation, membrane filtration, reverse osmosis, photocatalytic degradation, ion exchange, and advanced oxidation processes have been developed for the removal of antibiotics/other pharmaceutical residues and other organic pollutants from wastewater.[27,28] These methods, however, require expensive equipment, high-energy requirement, and/or continuous need of chemicals making them exorbitant and environmentally unfriendly.[4] It is therefore necessary to develop a simple, efficient, and affordable technology for the removal of antibiotics and other endocrine disrupting compounds (EDCs) in a bid to improve water quality, which may in turn improve the quantity of re-usable water.

Physicochemical technology such as adsorption offers a potentially cheaper and environment-friendly alternative for removal of organic contaminants in water. Adsorption has been reported to be an effective technique for the removal of various organic pollutants from contaminated water.[4,15] This method is simple in design, easy in operation, flexible, efficient, with capability of removing a wide range of pollutants.[4,15] Adsorbents such as activated carbons (ACs) have excellent removal efficiencies among various adsorbents that have been investigated for wastewater treatment.[28] ACs have high porosity, well developed internal surface area, enhanced surface properties, and improved adsorption capacity. However, application of commercially available ACs in large scale operations is infeasible due to their high cost. As a result, great effort has been extended in developing cost-effective ACs from renewable sources.[29] Agricultural and industrial wastes such as coconut shells,[30] peach stones,[31] macadamia nut shells,[4] and sewage sludge,[32] among others have been utilized effectively as cheap precursors of ACs. Moreover, the possible regeneration of the saturated adsorbent for potential reuse and their environment-friendly disposal is an added advantage to the adsorption process.[33]

Information about the availability and widespread occurrence of pharmaceuticals in the environment has been highlighted in America, Canada, and in many European and Asian countries.[14,34] However, information concerning the identification and quantification of pharmaceutical compounds in many African ecosystems is sparse and scanty. The capability of the sewage treatment processes in removing pharmaceuticals from wastewater in African countries is also not fully known.[5,14,35–36] There is scarcity of information concerning the utilization of grape slurry waste as a precursor of carbon-based adsorbents, as well as its application for the removal of amoxicillin (AMX), ampicillin (AMP), or chloramphenicol (CHLR).

Grape slurry from wine manufacturing is a major waste obtained from wine production. Thus, enormous quantities are readily available and accessible, although a small fraction is being used as manure. Grape slurry waste contains lignocellulose residues which confers desirable characteristics on it as a precursor for the production of ACs. This study therefore aimed at the monitoring of three antibiotic residues (AMX, AMP, and CHLR) in selected surface water; as well as prepare, characterize, and explore the effectiveness of ACs prepared from grape slurry waste, for abatement of the antibiotics' residues from aqueous solutions.

## 2. Experimental Section

### 2.1. Antibiotics Standards and Reagents

Neat standards of AMX, AMP, and CHLR (**Figure 1**) with purity >95% were obtained from Duchefa Biochemie, the Netherlands. Hydrochloric acid (HCl), methanol (MeOH), potassium hydroxide (KOH), and sodium hydroxide (NaOH) were purchased from Sigma–Aldrich, USA. Milli-Q water used in this study was produced in the laboratory in a Millipore RiOs instrument (Germany).

### 2.2. Preparation of Working Standards

A total of 0.01 g of AMX, AMP, and CHLR were each weighed and dissolved in 100 mL Milli-Q water to achieve 100 mg $L^{-1}$ stock solutions of the antibiotics. Each of the stock solutions was stored in a refrigerator at 4 °C and used within 48 h in order to minimize errors associated with possible analyte degradation. Working solutions of concentrations ranged between 5 and 100 mg $L^{-1}$ were prepared from the stock solutions prior to use.

Antibiotic-contaminated surface water were prepared in the laboratory by spiking distilled water with AMX, AMP, and CHLR to achieve a concentration of 30 mg $L^{-1}$ solution of each.

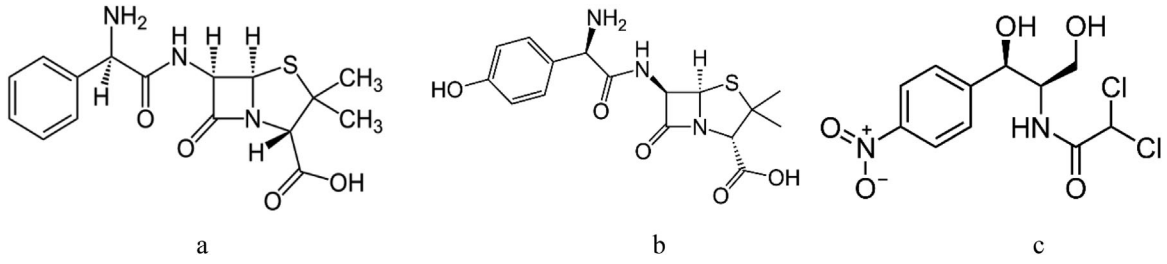


**Figure 1.** Structure of ampicillin ($C_{16}H_{19}N_3O_4S$; Fwt: 349.41 g $mol^{-1}$) (a), amoxicillin ($C_{16}H_{19}N_3O_5S$; Fwt: 365.4 g $mol^{-1}$) (b), and chloramphenicol ($C_{11}H_{12}Cl_2N_2O_5$; Fwt: 323.132 g $mol^{-1}$ (c).

### 2.3. Instrument Optimization

An ultra-high-pressure liquid chromatograph coupled to an ultraviolet-visible-diode-array-detector (UHPLC-UV-vis-DAD) was optimized for the separation, detection and quantification of AMX, AMP, and CHLR in aqueous matrix. The optimum instrument parameters were achieved by streaming 5 μL sample in a mobile phase composition consisting of 40% MeOH/water (v/v) (degassed), at a flow rate of 1 mL $min^{-1}$ through a C18 Agilent column (150 × 4.6 mm id, 5 μm), at isothermal column temperature of 30 °C, and detection wavelength of 210 nm.

### 2.4. Analyte Recovery

Solid phase extraction (SPE) was optimized for the recovery of AMX, AMP, and CHLR from simulated wastewater spiked with 0.03 g $L^{-1}$ antibiotic and from surface water samples, using hydrophilic/lipophilic balance (HLB) cartridges (Oasis, 500 mg, 6 mL). Prior to analyte extractions, the HLB cartridges were conditioned using 6 mL of absolute methanol (MeOH) followed by 6 mL Milli-Q water. After conditioning the cartridges, 30 mL aliquots of the simulated wastewater of varying analyte concentrations were loaded on the cartridges and eluted at a flow rate of 2 mL $min^{-1}$. Thereafter, the analyte retained on the cartridge was extracted in two cycles by eluting with 6 mL MeOH. The MeOH extracts were concentrated to dryness under nitrogen stream and re-constituted in 2 mL 50% MeOH (MeOH/water, 50:50, v/v). All samples were filtered through 0.45 μm nylon fiber filters into 2 mL vials for analysis.

The percentage of the recovered standard was determined by comparison of results with the spiked concentrations. The optimized recovery procedure was used for the recovery of the antibiotics from the surface water samples.

### 2.5. Sampling of Surface Water

Surface water samples were pooled into 2.5-L amber colored glass bottles, along the mainstream transects drainage stretch of the Diep River at different sampling points (P1–P5) (**Table 1**), between the geo-reference coordinates −33.801359 S and 18.535580 E and −33.881853 S and 18.489755 E, over two seasons, that is, winter and spring.

The pH, conductivity, temperature, and total dissolved solids (TDS) of the water samples were measured and recorded in situ using a pre-calibrated pH meter (HANNA, HI 991300). The collected water samples were kept in an ice chest as recommended by Nikolaou et al.[37] for onwards transfer to the laboratory for analysis. The samples were processed using SPE to concentrate and analyzed within 48 h of sample collection as recommended by Gulkowska et al.[38]

### 2.6. Preparation of Adsorbents

Grape slurry waste, a bio-organic waste from wine production was collected from a wine plant in Stellenbosch, Western Cape, South Africa. The raw grape slurry waste was washed with distilled water, dried under ambient conditions, sorted, and pulverized to fine aggregates (particle size ≤250 μm). The pulverized particle aggregates were subjected to carbonization in a muffle furnace (Gallenkamp) at 650 °C for 2 h under nitrogen stream. In order to enhance the adsorption capacity of the carbonized grape slurry, the carbonized aggregates were mercerized and modified by soaking in 1.5 M HCl and 1.5 M KOH for 6 h to produce the acid modified adsorbent (GSA) and the base modified adsorbent (GSB), respectively. The HCl and KOH treated adsorbents were afterwards washed with distilled water to near neutral pH, and dried in an oven (Scientific, Series 9000) at 100 °C for 6 h.

### 2.7. Characterization of Adsorbents

The untreated grape slurry waste (GS) and activated carbons (GSA and GSB) were characterized using Fourier transform infra-red (FTIR) spectrometry and scanning electron microscopy (SEM). Energy dispersive X-ray (EDX) (Zeiss EVO MA15 Scanning Electron Micro analyser, USA) was also used to determine the elemental and phase compositions of untreated biomass of GS and activated carbons (GSA and GSB) produced from grape slurry waste.

### 2.8. Fourier Transform Infrared Spectroscopy (FTIR)

Functional group evaluation of the untreated biomass (GS) and the activated carbons (GSA and GSB) were investigated using FTIR spectrometry (Perkin Elmer, Spectrum 1000, UK). About 0.02 g of the dry adsorbents prepared from the grape slurry biomass were placed on the silver surface cavity of the FTIR spectrometer at ambient conditions and analyzed using a diamond needle. Each of the adsorbents was scanned between 4000 and 400 $cm^{-1}$ at an average of three scans, with resolution of 4 $cm^{-1}$.

**Table 1.** Description of sampling locations.

| Sampling point | Latitude | Longitude | Site description |
|---|---|---|---|
| P1 | −33.801359 S | 18.535580 E | Upstream flow from veld/farms |
| P2 | −33.834589 S | 18.522147 E | Stream flow at table view |
| P3 | −33.837625 S | 18.519621 E | Stream flow beyond WWTP point of discharge |
| P4 | −33.847279 S | 18.512020 E | Industrial discharge |
| P5 | −33.881853 S | 18.489755 E | Downstream (proximity to ocean; marine water intrusion: Biome) |

### 2.9. Scanning Electron Microscopy (SEM)

The characteristics of the surface morphologies of the untreated biomass (GS) and the activated carbons (GSA and GSB) before and after the adsorption process were studied by SEM (Zeiss EVO MA15, Scanning Electron Micro analyser, USA) operated at 10–25 kV. During sample preparation for SEM analysis, a thin layer of adhesives serving as carbon glue was attached onto a stub, and very little amount of the samples to be analyzed was spread on the stub materials and subsequently viewed on the instrument to obtain micrographs.

### 2.10. Energy Dispersive X-Ray (EDX) Elemental and Phase Compositions Analysis

Elemental and phase compositions analysis of the adsorbents were done by SEM. Qualitative assessment/analysis was achieved by the application of secondary electron images of X-radiation onto gold coated samples, while quantitative analysis was performed by EDX spectroscopy on-line (Oxford Instruments, X-Max) 20 $mm^2$ detector, programmed with an Oxford INCA software. Gold coating was employed on the sample surface in order to achieve highly polished surfaces as well as to improve surface conductivity. As a quality assurance protocol, pure cobalt was used periodically to correct any slight or major detector drifts.

### 2.11. Adsorption Experiments

In order to study the effect of different controlling parameters such as adsorbent dose, pH, contact time, and initial concentration, on the adsorption capacity of the grape slurry adsorbents for AMX, AMP, and CHLR, batch sorption experiments were carried out in 100 mL Erlenmeyer flasks. Simulated wastewater (25 mL) containing 30 mg $L^{-1}$ of AMX, AMP, and CHLR was prepared. A fixed amount of adsorbent (0.10 g) was added into 100 mL flasks containing 25 mL aliquots of the antibiotics, thoroughly mixed and then agitated on an orbital shaker at 150 rpm at room temperature ($23 \pm 2\,^{\circ}C$). All samples were withdrawn after a definite time interval and filtered through 0.45 μm Acrodisc GHP membrane syringe filter (25 mm). The residual concentrations of the antibiotic solutions were determined using HPLC-UV-DAD (Shimadzu, Japan) after SPE. Control samples were simultaneously run with the experimental samples to correct for any possible deviations that might occur during the adsorption processes. All tests were performed in triplicate.

The adsorption capacities, $q_e$ (mg $g^{-1}$) and percentage removal, $y$, of the antibiotics at equilibrium using the activated carbons were calculated using Equation (1) and (2), respectively:

$$q_e = \frac{(C_o - C_e)}{w} v \quad (1)$$

$$y = \frac{(C_o - C_e)}{w} \times 100 \quad (2)$$

where $q_e$ is the equilibrium adsorption capacity (mg $g^{-1}$) of the adsorbent for the adsorbate; $c_o$ and $c_e$ are the initial and residual concentrations (mg $L^{-1}$) of antibiotics in solution, respectively; $w$ is the mass (g) of the activated carbons; and $v$ is the volume (L) of the solution.

To assess the effect of adsorbent dose on antibiotics removal from simulated wastewater, various doses of the adsorbent (0.10–0.40 g) were added to 25 mL of the antibiotic solutions (30 mg $L^{-1}$ AMX, AMP, and CHLR). The solutions were agitated on a mechanical shaker at 120 rpm and room temperature, neutral pH, and 150 min.

For pH effect, an initial antibiotics concentration of 30 mg $L^{-1}$ with adsorbent dose of 0.10 g over a pH range of 4–12 were placed on an orbital shaker at 120 rpm at room temperature for 150 min. 0.10 M KOH and 0.10 M HCl were employed to adjust the pH of the solutions.

Kinetic studies were performed to investigate the adsorption rate and interaction of the adsorbents. Activated carbons (0.10 g) were weighed accurately into 100 mL Erlenmeyer flasks containing 25 mL simulated wastewater (30 mg $L^{-1}$ of each antibiotic, respectively). Supernatants were collected at a predetermined time interval ranging from 30 to 300 min, and the concentrations of the antibiotics analyzed to determine the quantity of the antibiotics adsorbed, $q_t$ (mg $g^{-1}$) at the different time intervals using Equation (3).

$$q_t = \frac{(C_o - C_t)v}{m} \quad (3)$$

where $c_o$ and $c_t$ (mg $g^{-1}$) is the liquid-phase concentrations at initial and at time intervals, $v$ is the volume (L) of the solution, and $m$ is the mass (g) of adsorbent.

Adsorption isotherms were carried out with different initial concentrations of antibiotics (30–100 mg $L^{-1}$) while maintaining the grape slurry adsorbent dosage at a constant level (0.10 g) for 150 min at room temperature.

## 3. Results and Discussion

### 3.1. Optimization and Validation of HPLC-UV-Vis Method

The chromatogram of the standard cocktail mix of AMX, AMP, and CHLR is presented in **Figure 2**. The chromatogram shows good separation. The retention times of the antibiotics, AMX, AMP, and CHLR were 1.61, 2.60, and 8.08 min, respectively. Thereafter, subsequent identification and quantification of the antibiotics was achieved by external calibration.

The response factor of individual antibiotic to the individual internal standard was measured and calculated at least three times at the beginning, in between and at the end of each batch of five injections.

Mobile phase characteristics was varied in order to facilitate efficient baseline separation and detection of the antibiotics, by varying the percentage composition of MeOH and MilliQ water, adjustment of the mobile phase optimal pH, the flow rate and column temperature. The optimum conditions were 40% MeOH/water (v/v), at a flow rate of 1 mL $min^{-1}$; column

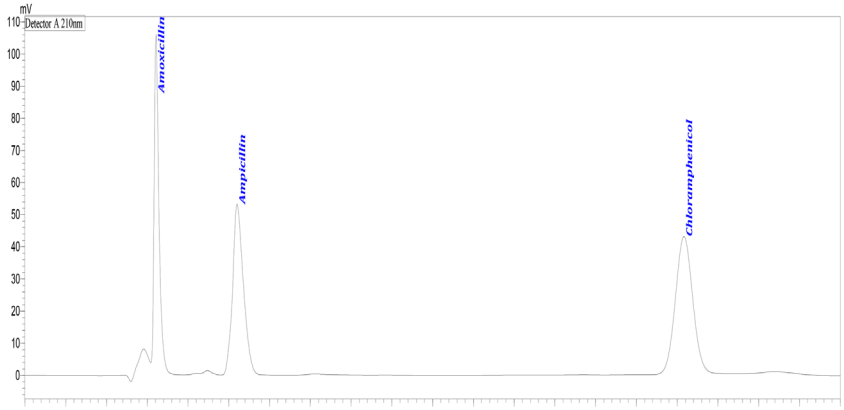


**Figure 2.** Chromatogram of AMX, AMP, and CHLR.

**Table 2.** Linear regression parameters for AMX, AMP, and CHLR standards.

| Standard | Linear regression equation | Retention time [min] | $R^2$ | $\lambda_{max}$ [nm] | LOD [mg $L^{-1}$] | LOQ [mg $L^{-1}$] |
|---|---|---|---|---|---|---|
| AMX | $y = 21\,347x + 21\,709$ | 1.61 | 0.9999 | 210 | 0.29 | 0.86 |
| AMP | $y = 11\,949x - 12\,397$ | 2.60 | 0.9998 | 210 | 0.19 | 0.58 |
| CHLR | $y = 14\,707x + 8589$ | 8.08 | 0.9998 | 254 | 0.22 | 0.67 |

temperature of 30 °C; with mobile phase MeOH/MilliQ water varying between 20:80 to 60:40.

The linear fit curve was plot plotted using the least square method, while the International Council of Harmonization (ICH) performance parameters were calculated to ascertain the system suitability of the method, for the extraction/recovery and determination of AMX, AMP, and CHLR in aqueous matrices. The instrument response to the detection of each of the β-lactam antibiotics showed linear sensitivity to increasing concentrations with coefficient of correlation ($R^2$) values >0.999 for all three analytes (**Table 2**).

Replicates of blank solutions were analyzed, and their signals recorded, followed by gradient of working standard solutions. Least square regression analysis for the method was carried out for the slopes and intercepts obtained from response signals of gradient of working standard solutions for each of the antibiotics in order to ascertain the method's limit of detection (LOD) and limit of quantification (LOQ) values. The LOD and LOQ values were 0.29 and 0.87 mg $L^{-1}$, 0.19 and 0.57 mg $L^{-1}$, and 0.22 and 0.67 mg $L^{-1}$ for AMX, AMP, and CHLR, respectively.

### 3.2. Recovery Studies of Analytes Using SPE

The efficiency of quantitative recoveries of the antibiotics using SPE were evaluated by extracting AMX, AMP, and CHLR from MilliQ water (solutions) spiked at three levels (20, 50, and 100 mg $L^{-1}$) with cocktail of the antibiotics. The relative percentage recovery of the antibiotics ranged between 95% and 102% for AMX, 88–99% for AMP, and 93–103% for CHLR (**Table 3**).

The results showed that affinity of the HLB SPE cartridges for the analytes was high, with the precision (expressed as relative standard deviation [RSD]), ranging from 0.27% to 1.89%. This implies that the SPE method has enhanced extraction efficiency for the recovery of the analytes from aqueous matrices.

### 3.3. Analysis of Surface Water Samples

The chromatogram of the antibiotics extracts from the simulated surface water and the surface water collected from Diep River were also analyzed along with control samples (blank), in order to correct for the target analytes. The recoveries of antibiotics were evaluated by the use of reference standards of the antibiotics containing AMX and CHLR, since most β-lactam antibiotics behave in a similar

**Table 3.** Mean recovery percentages for AMX, AMP, and CHLR by the SPE method.

| Standard | Concentration [mg $L^{-1}$] | Measured concentration [mg $L^{-1}$] | RSD [%] | Average recovery [%] |
|---|---|---|---|---|
| AMX | 20 | 18.93 | 1.31 | 94.65 |
| | 50 | 49.01 | 1.89 | 98.02 |
| | 100 | 102.03 | 1.06 | 102.03 |
| AMP | 20 | 17.58 | 1.27 | 87.90 |
| | 50 | 48.64 | 0.63 | 97.28 |
| | 100 | 99.46 | 0.48 | 99.46 |
| CHLR | 20 | 18.54 | 1.39 | 92.70 |
| | 50 | 49.88 | 0.27 | 99.76 |
| | 100 | 103.36 | 0.92 | 103.36 |

fashion during extraction and analysis. The recoveries of the antibiotics varied from 83.72% to 94.96% and relative standard deviation (RSDs) ranged between 3.56% and 14.60%.

Amoxicillin was the most prevalent among the investigated antibiotics; detected at nearly all the sampling points with concentrations reaching a maximum of $5.84 \pm 0.08\,\mu g\,L^{-1}$ during winter and $11.55 \pm 0.04\,\mu g\,L^{-1}$ during spring. The widespread occurrence and distribution of AMX in all the surface water samples may be connected to discharges from domestic and industrial sources as well as WWTP effluent into the Diep River. AMP was detected only in sampling station (P5) during the two seasons, with concentrations reaching a maximum of $1.24 \pm 0.24$ and $5.27 \pm 0.06\,\mu g\,L^{-1}$ during winter and spring, respectively. The detection of AMP at P5 may be attributed to accumulation, since the sampling point is located along the lower drainage toward the estuary. The intrusion of saline marine water from the sea into the estuarine ecosystem probably also facilitates the stabilization of the antibiotics due to high water salt content. CHLR did not occur at detectable levels at all the sampling points. The reason for this is not very clear. Some reports have suggested that CHLR easily degrade via hydrolysis in water at pH values in the range of 2–8. According to Huang and Sedlak[39] and Nie et al., [40] the concentrations of most β-lactam antibiotics are not expected to be high in surface water, since they are prone to hydrolytic degradation over a period of time. Thus, the non-detection of CHLR and the low concentrations of the investigated antibiotics may be due to hydrolytic degradation, at surface water pH ranging between 7.01 and 7.81 across all sampling stations. In general, the concentrations of the antibiotics were high at sampling stations P5. The higher values may be attributed to fractional accumulations of the compounds from upstream, over time.

### 3.4. Proximate Elemental Composition of Grape Slurry Carbon

The optimum condition for the carbonization of grape slurry was at charring temperature of 650 °C for 120 h. Biomass weight of 20 g yielded 8.97, 7.67, and 7.06 g at 450, 550, and 650 °C, respectively. According to Fagbayigbo et al.,[41] the reduction in weight of the carbonized product at temperatures >600 °C may be due to enhanced aromatization processes of the biochar.

Chemical activation of the carbon was optimized with 1.5 M HCl and KOH, producing a dark black carbon. KOH activation probably resulted in well-developed pore structured ACs with improved quantities of micropores and mesopores on the surface. This observation is consistent with the findings of Xu et al.[42] and Fagbayigbo et al.[41] GSA had the highest maximum carbon content (89.11%) and the least oxygen content (9.04%) compared to GSB and GS which gave carbon contents of 82.40% and 56.56% and oxygen contents of 13.62% and 33.93%, respectively.

### 3.5. Adsorbent Characterization

#### *3.5.1. Surface Characteristics of Carbon Samples*

Chemical activation of adsorbent with HCl reduces the pH of the solution with a possible tendency to enhance adsorption process viz-a-viz electrostatic attraction. On the contrary, chemical activation of adsorbent with KOH increases the solution pH; thus, suggesting the predominance of the basic −OH group on the surface of the AC. The predomination of surface charges at acidic or basic pH may induce selectivity thereby enhancing electrostatic interactions toward positively or negatively charged ionic molecules or compounds.[41,43,44] Raw untreated grape slurry waste was generally neutral.

#### *3.5.2. Physicochemical Properties of Grape Slurry Adsorbents*

The moisture content of the HCl modified (GSA) and KOH modified (GSB) adsorbents were 10.48 and 13.28%, respectively, while that for the untreated biomass was 23.38% (**Table 4**). The ash content and organic matter content of GSA, GSB and the untreated adsorbents were 6.75%, 7.32%, and 22.60%, respectively, and 93.25%, 92.68%, and 77.40%, respectively, while the pH values were 5.27, 9.17, and 6.61, respectively.

Biomass and sorbent materials with low moisture, low ash, and high organic matter content have been reported to be excellent adsorbents due to their indication of relatively small particle density.[45] Where this assertion is true, then the acid modified activated grape slurry carbon adsorbents is expected to show better sorption potential, followed by the base modified activated grape slurry carbon adsorbents, and then the untreated adsorbent. Thus, adsorbent GSA with moisture, ash and organic matter content of 10.48%, 6.75%, and 93.25%, respectively, and GSB with moisture, ash and organic matter content of 13.28%, 7.32%, and 92.68%, respectively, are expected to show better performance, and preferable for adsorption compared to GS with the higher moisture and ash content (23.38% and 22.60%, respectively). Ayanda et al.,[46] Fatoki et al.,[47] and Ekpete et al.[45] explained that differences in the final pH, moisture, ash, and organic matter content of activated carbonized adsorbents and the untreated biomass may be attributed to the carbonization and activation processes which to a large extent may have resulted in the elimination of all non-carbon materials, in contrast the untreated biomass.

The ignition point of carbon in an adsorbent is strongly influenced by its ash content, and this depends on the relative composition of organic matter content of the adsorbent. According to Ekpete et al.[45] and Ekpete and Horsfall,[48] the ignition point of adsorbent carbon is an important factor when considering their use for adsorption of aqueous solutions. This is because high ash content reduces the overall activity of AC, and the efficiency of reactivation, hence, the lower the ash value, the better the adsorbent capacity of AC. Abdullah et al.[49] reported that ash content values suitable for the use of carbon for

**Table 4.** Physicochemical properties of GSA, GSB, and GS.

| Characteristics | GSA | GSB | GS |
|---|---|---|---|
| pH | 5.27 | 9.17 | 6.61 |
| Moisture content (%) | 10.48 | 13.28 | 23.38 |
| Ash content (%) | 6.75 | 7.32 | 22.60 |
| Organic matter content (%) | 93.25 | 92.68 | 77.40 |

absorption should be within a range of 1–20%, thus GSA and GSB with ash content within this values may have good sorption potential.

### 3.5.3. FTIR Analysis

Characteristic functionality or chemical functional groups present in biomass used as adsorbents partly provides an insight into the mechanism involved in the adsorption process. The FTIR spectra pattern of GS, GSA, and GSB presented in **Figure 3** showed the characteristic bands of the available functional groups in the different adsorbents.

The strong absorption at 2920.77 $cm^{-1}$ in the spectra of the untreated biomass could be attributed to asymmetric C–H stretching vibration of methyl ($CH_3$) group, and symmetric C–H stretching vibration of methylene ($CH_2$) group of the precursor. Absorption in this region was eliminated in the spectra pattern of carbonized and acid activated GSA, and base activated GSB. This may be due to the occurrence of chemical transformation during the carbonization and activation processes.[41–42,45] Furthermore, C–H bonding of aromatic structures present in the adsorbents may overlap with those that are from aliphatic chains or other groups present.[50] The weak O-H absorption at 3240.85 $cm^{-1}$ in the spectra pattern of GSB may be attributed to residues of KOH solution used for its modification/activation. Zhang and Chuang[51] reported similar observation for adsorbent materials modified with NaOH or KOH. Sharp absorption bands observed in the untreated biomass at 1818.44 and 1032.56 $cm^{-1}$ is attributed to C═O, C-C(O)-C, and C-O functional groups stretching vibrations. In GSA and GSB These vibrational stretching bands shifted slightly to 1590–1700,

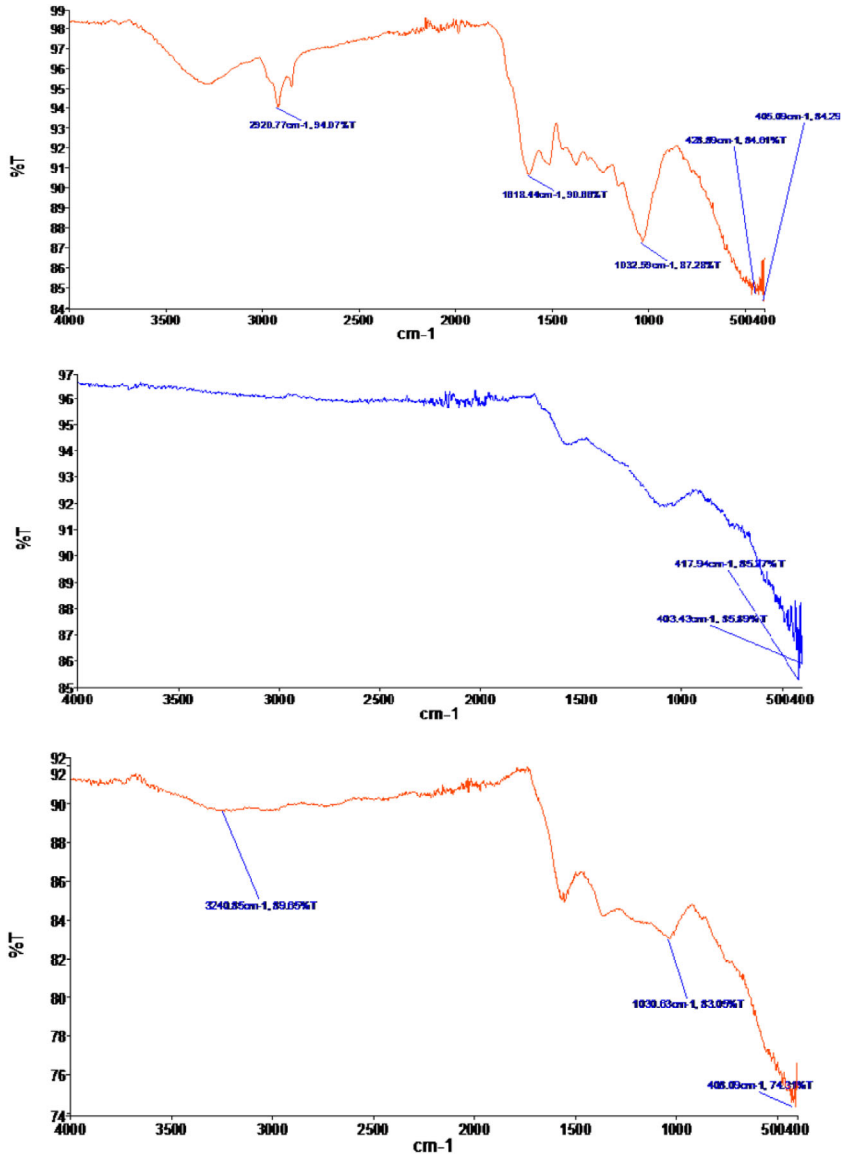


**Figure 3.** FTIR spectrum for a) untreated biomass (GS), b) HCl-activated carbon (GSA), and c) KOH-activated carbon (GSB).

1100–1320, and 1030.63 $cm^{-1}$ in the spectra patterns of GSA and GSB, which are characteristic vibrational stretches of asymmetric C=O of carbonyls or symmetric C-C; C=C alkene groups and C-O functional groups, respectively. The shift of the absorption bands at these wavelengths suggests the deformation and/or destruction of functional groups present on the adsorbent during carbonization and chemical activation.[52–54] Two weak peaks of absorption were noted at 426.19 and 405.09 $cm^{-1}$ in GS, at 417.94 and 403.43 $cm^{-1}$ in GSA, and at 406.09 $cm^{-1}$ in GSB.

### 3.5.4. SEM Analysis

Micrograph images obtained from SEM of the adsorbents GSA, GSB, and GS before and after adsorption are presented in **Figure 4**. The SEM images of GSA and GSB revealed that they are smooth surfaced with well-developed pore structures. The surface morphology of GSA before sorption appeared as a cluster of smooth needle/fibrous-like particulates with well-defined and open pore spaces of different size ranges (Figure 4a), while the morphology of GSB are of clustered crystalline grain structures of rhombohedral to polygonal shape (Figure 4c). The morphology of the untreated biomass (GS) was mostly of distorted crystalline particles, fussed together at the center (Figure 4d). An examination of the micrograph of GS surface morphology indicate probable octahedral particles, with no clearly defined pore spaces; hence, the internal surfaces of the adsorbent material (GS) might not be accessible, limiting intra-particle diffusibility of the fluid due to closed porosity. Xie et al.[54] noted that the smooth surfaces of activated carbon materials may be resultant of the transformation of the plant lignin-cellulose, which arises as a result of the deconstruction of the plant cells. Similar morphologies have been previously reported for a number of adsorbents produced from plant biomasses.[55–57]

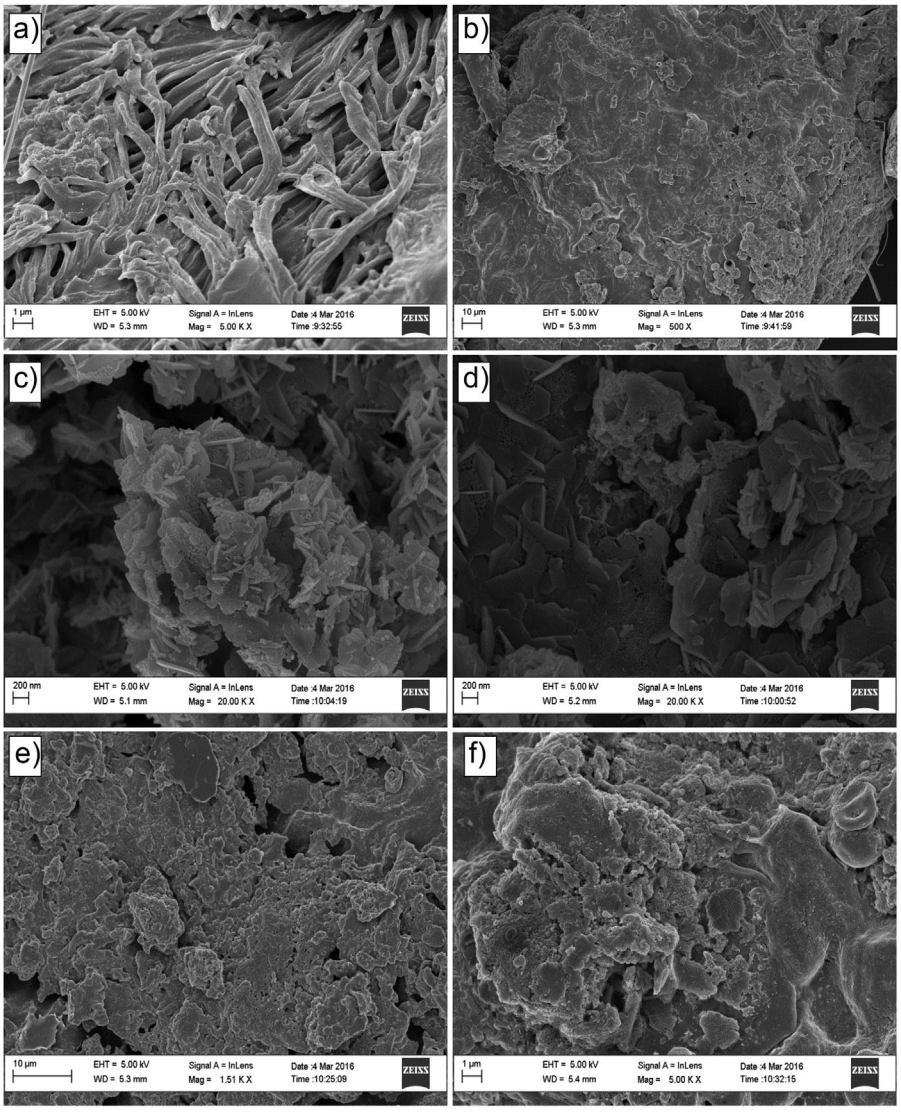


**Figure 4.** SEM images of GSA a) before and b) after adsorption; GSB c) before and d) after adsorption; and GS e) before and f) after adsorption.

After adsorption, the surface texture of the adsorbents was altered. This was assumed to be as a result of the accumulation of antibiotics on the adsorbents during the adsorption process, where the adsorbates penetrate the inner pore spaces and adsorbent surface until saturated. Zhang et al.[58] also suggested that adsorbed compounds may replace existing molecules on the surface of the adsorbents during adsorption.

### 3.6. Adsorption, Kinetics, and Thermodynamics of the Sorption of AMX, AMP, and CHLR Onto Grape Slurry Activated Carbon Adsorbents

#### 3.6.1. Effects of Adsorbent Dose

The effectiveness of removal of contaminants from aqueous matrices partly depends on the capacity of the adsorbent to sorb the contaminants, quantity of the adsorbent, and the extent to which the matrix is contaminated. Adsorbent dose is critical in determining the sorption efficiency of adsorbents at any given initial concentration of adsorbates in aqueous solutions.[41] The effect of adsorbent dose on the removal of the selected antibiotics is shown in **Figure 5**. The result for the removal of the antibiotics increased with increasing GSA and GSB adsorbent doses. An optimum adsorption threshold was reached for both adsorbents at an adsorbent dose of 0.4 g. At initial, a linear relationship between adsorbent dose and quantity of adsorbate adsorbed was observed, until the absorbents dose of 0.4 g. A similar trend was reported in studies, suggesting an enhanced sorption at higher adsorbent doses.[41,59]. There was a remarkable sorption of AMX, AMP and CHLR at adsorbent dose of 0.4 g with sorption percentages of 75.46, 72.51, and 72.69, respectively, onto GSA, and 87.10, 73.77, and 91.08, respectively, onto GSB; in contrast to lower adsorbent dosage (0.1 g) which gave lesser percentage removal (<40%) for the antibiotics with both adsorbents. However, sorption onto GSB was better than on GSA.

The enhanced adsorption yields with increasing adsorbent dose may be due to availability of more active binding sites with an increase in adsorbent dose. According to Hameed et al.,[60] increasing adsorbent dosage increases the surface area available for sorption of adsorbate molecules. Therefore, a fixed dose of adsorbent can only adsorb a certain amount of adsorbate; thus, increase in adsorbent dose would result in an increase in the quantity of the adsorbate.

#### 3.6.2. Effect of Contact Time

The optimum contact time for adsorbates removal onto the adsorbents was evaluated over a time range of 30–300 min. The results presented in **Figure 6** show the contact time required to reach equilibrium for the adsorption of the antibiotics onto the adsorbents. The sorption of AMX onto both adsorbents attained equilibrium at 120 min; while the sorption of AMP onto GSA and GSB reached equilibrium at 150 and 90 min, respectively. The equilibrium attainment for adsorption of CHLR onto GSA was the fastest, at 90 min, while the time required to reach equilibrium was the slowest for the sorption of CHLR onto GSB (150 min).

Steep slopes indicating high rates of adsorption of the antibiotics onto the adsorbents were observed in the initial stages of the sorption processes prior to the attainment of equilibrium. This could be due to the surface density of available binding sites on the sorbent materials. At equilibrium, the active sites became occupied resulting in lesser sorption of the adsorbates.[60] This is because on attainment of equilibrium, there is an increase in the repulsive forces between the sorbent molecules and the bulk phase, thereby pushing the adsorption process toward equilibrium. Further increases in contact time after equilibrium did not result in significant differences in sorption capacities of the adsorbents for all three antibiotics.

The variable equilibrium contact times obtained for the different adsorbates with the various adsorbents were used as the optimum contact times in further studies. For an initial concentration of 5 mg $g^{-1}$ of the individual adsorbate solutions, a maximum sorption capacity corresponding to 2.971, 2.838, and 3.104 mg $g^{-1}$ for AMX, AMP, and CHLR, respectively, was achieved using GSA.

#### 3.6.3. Kinetics of Sorption

The mechanism of the adsorption of AMX, AMP, and CHLR onto GSA and GSB, and the rate limiting step for the process was estimated using the kinetic models from which the rate

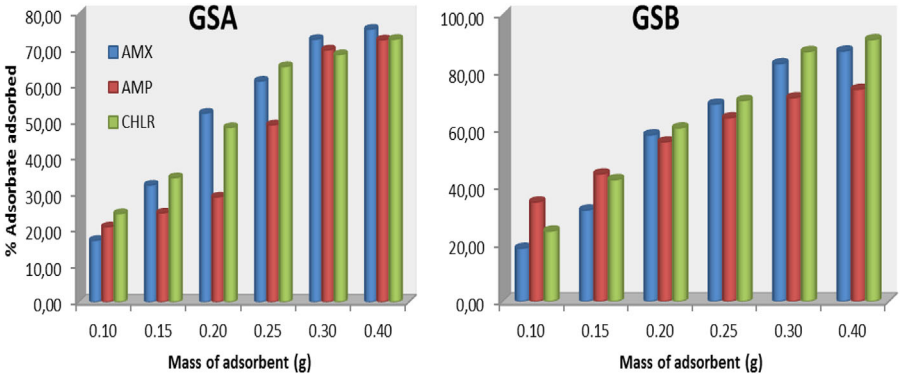


**Figure 5.** Percentage removal of adsorbates onto GSA, GSB, and GS. Experimental conditions: concentration of adsorbates = 30 mg $L^{-1}$; volume of adsorbates solution = 25 mL; stirring speed = 120 rpm; temperature = 20°C.

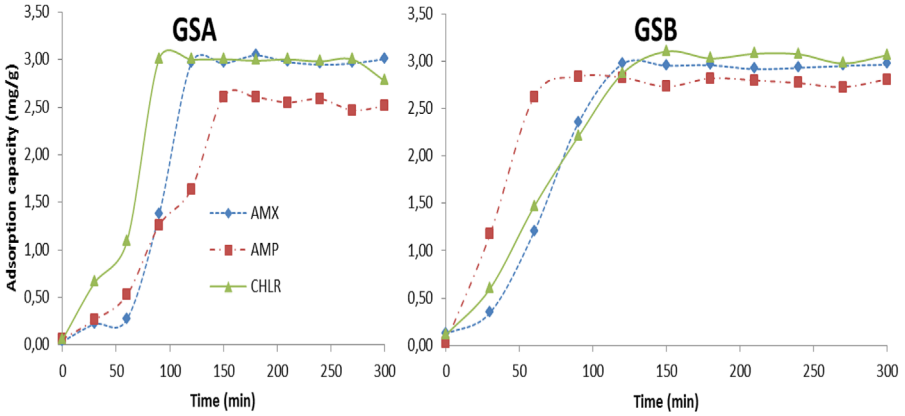


**Figure 6.** Effect of contact time on adsorbates' adsorption onto GSA and GSB. Experimental conditions: concentration of adsorbates = 30 mg $L^{-1}$; volume of adsorbates solution = 25 mL; mass of adsorbent = 0.10 g; stirring speed = 120 rpm; temperature = 20 °C.

constants for the pseudo-first order, pseudo-second order and the Elovich kinetic models were determined.

*The pseudo-first-order model*: The linearized form of the pseudo-first order model was applied.[61] It is generally presented as

$$\log(q_e - q_t) = \log q_e - \frac{k_1}{2.303}t \quad (4)$$

where $q_e$ is the amount of AMX adsorbed at equilibrium (mg $g^{-1}$) per unit weight of adsorbent, $q_t$ is the amount of sorbate (antibiotics) adsorbed (mg $g^{-1}$) at a time $t$, and $k_1$ (obtained from the slope of the linear plot of $\log(q_e - q_t)$ vs. $t$) is the kinetic rate constant ($min^{-1}$) of pseudo-first order kinetics.

*The pseudo-second-order model*: The linear expression of the pseudo-second order equation[62] presented in Equation (5), was used to determine $k_2$ and other model parameters.

$$\frac{t}{q_t} = \frac{1}{k_2 q_e^2} + \frac{t}{q_e} \quad (5)$$

$k_2$ is the rate constant (g $mg^{-1}$ $min^{-1}$) of the pseudo-second order model. Applying Equation (4) to the adsorbate adsorption process, allows for determination of $q_e$ and $k_2$ can be from the slope and intercept of the plot $t/q_t$ versus $t$, respectively.

*The Elovich equation*: The Elovich equation has been used to describe the adsorption of a number of pollutants from aqueous solutions[63,64] and in its simplest form is expressed as

$$q_t = \frac{1}{B}\ln(A_\varepsilon B) + \frac{1}{B}\ln(t) \quad (6)$$

where $q_t$ is the amount (mg $g^{-1}$) of adsorbate adsorbed at a time $t$, $A_\varepsilon$ is the initial adsorption rate (mg/g/min) and $B$ is the desorption constant (g $mg^{-1}$). Linearity of a plot of $q_t$ versus ln$t$ describes a fit to the equation.

The results and parameters obtained from the kinetic models for the pseudo-first order, pseudo-second order, and the Elovich kinetic model are presented in **Table 5**.

The correlation coefficients ($R^2$) obtained from the pseudo-second order for the adsorption of the three adsorbates onto GSA and GSB are higher than the correlation coefficients of the pseudo-first order and the Elovich model. This indicates that the sorption of the three antibiotics onto the adsorbents was better described by pseudo-second order reaction. According to Zhang et al.,[65] pseudo-second order kinetic model assumes that the rate limiting step of sorption processes tend toward chemisorption. Thus, the sorption of the antibiotics onto the adsorbents may probably be a chemisorption process, although other mechanisms might also spike selective influences on the sorption process. The sorption of the antibiotics AMX, AMP, and CHLR onto the adsorbents, GSA and GSB, is therefore predominantly pseudo-second order processes. The removal of the adsorbate molecules from solution proceeds via chemical interactions/bonding with the adsorbents. Since $R^2$-values of both pseudo-first order and Elovich models were >0.5 except AMX on GSA, physisorption, and intra-particle diffusibility may selectively contribute to the sorption process.

**Table 5.** Kinetic model parameters for adsorbate adsorption onto GSA and GSB.

| | AMX | | AMP | | CHLR | |
|---|---|---|---|---|---|---|
| Model | GSA | GSB | GSA | GSB | GSA | GSB |
| Pseudo-first-order | | | | | | |
| $k_1$ ($min^{-1}$) | 0.02 | 0.02 | 0.02 | 0.013 | 0.02 | 0.02 |
| $q_e$ (mg $g^{-1}$) | 4.11 | 3.11 | 2.85 | 0.89 | 4.58 | 3.95 |
| $R^2$ | 0.3121 | 0.8274 | 0.8050 | 0.8157 | 0.7842 | 0.7137 |
| Pseudo-second-order | | | | | | |
| $k_2$ (g $mg^{-1}$ $min^{-1}$) | $0.07 \times 10^{-4}$ | 0.02 | 0.001 | 0.03 | 0.004 | 0.004 |
| $q_e$ (mg $g^{-1}$) | 3.02 | 4.67 | 2.66 | 2.93 | 3.24 | 3.21 |
| $R^2$ | 0.9879 | 0.9447 | 0.9969 | 0.9851 | 0.8174 | 0.9818 |
| Elovich | | | | | | |
| $A_\varepsilon$ | 0.03 | 0.03 | 0.03 | 0.06 | 0.04 | 0.05 |
| $B$ | 1.57 | 1.67 | 1.92 | 1.90 | 1.67 | 1.65 |
| $R^2$ | 0.6342 | 0.7548 | 0.6760 | 0.8780 | 0.7495 | 0.8111 |

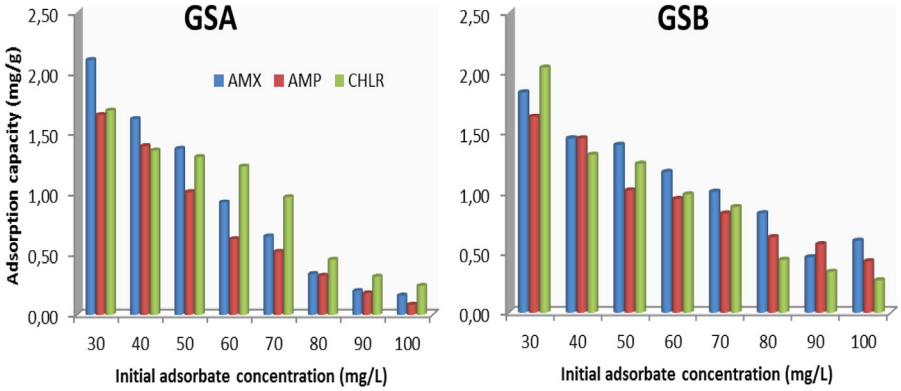


**Figure 7.** Sorption capacity of adsorbates by GSA and GSB at various initial adsorbate concentrations. Experimental conditions: volume of adsorbate solution = 25 mL; mass of adsorbent = 0.1 g; stirring speed = 120 rpm; temperature = 20 °C.

### 3.6.4. Effect of Initial AMX Concentration

Effectiveness of the adsorption process is a function of the rate of adsorption and the initial concentration of the adsorbates.[59] The effect of initial concentrations of adsorbed antibiotics onto the grape slurry ACs is presented in **Figure 7**. The affinity of adsorbent GSA for AMX was higher; hence, AMX was better removed from solution using GSA compared to AMP and CHLR, while GSB had a better affinity for CHLR.

There was a decrease in the removal of the antibiotics with increase of the antibiotics' concentration from 30 to 100 mg $L^{-1}$. Thus, an inverse relationship between sorption capacity of the adsorbents and the initial concentration of the antibiotics was observed, which indicates that lower initial concentration generally favored the antibiotics adsorption processes in aqueous solutions. The drop-in adsorption efficiency probably arose from the attainment of saturation due to the exhaustion of vacant surface binding sites at a high antibiotic concentration, since all adsorbents only have a limited number of active sites that may become saturated. Initial concentration therefore appears to be of little relevance in a batch process. Moussavi et al.[33] reported that, as long as adsorbent concentration remains constant during sorption (adsorbent mass/volume of solution), a decrease in the adsorption capacity with increased initial adsorbate concentration is related to limited availability of adsorption sites for an increased amount of adsorbate molecules.

In order for adsorption process to reach sorption equilibrium, the amount of adsorbed molecules will depend on conditions such as the initial adsorbate concentration and the driving force to overcome resistance of mass transfer for adsorbates, with the number of available adsorption sites being a limiting factor.[66] Furthermore, at sorption equilibrium, the amount of adsorbed molecules depend on conditions such as the initial adsorbate concentration and the driving force to overcome resistance of mass transfer for adsorbates, with the number of available adsorption sites being a limiting factor.

*Adsorption isotherms*: Adsorption isotherms which describe equilibrium and adsorption behavior of adsorbates (solutes) onto the surface of adsorbents (solid phase) at optimized pH and temperature, are very critical for the optimization of the adsorption system. Sorption performance and efficiency (amount of adsorbates removed) of adsorbents could also be evaluated from adsorption isotherm models. Three adsorption equilibrium isotherms namely the Langmuir, Freundlich, and Temkin isotherm models were used to test the experimental data generated in this study.

The linearized form of the Langmuir model is represented by Equation (7).

$$\frac{C_e}{q_e} = \frac{1}{q_{max} K_L} + \frac{C_e}{q_{max}} \tag{7}$$

$C_e$ represents the equilibrium concentration (mg $L^{-1}$) of adsorbates in solution, $q_e$ represents the amount of adsorbate adsorbed per gram of the adsorbent at equilibrium (mg $g^{-1}$), $q_{max}$ represents the maximum monolayer coverage capacity (mg $g^{-1}$), and $K_L$ is the Langmuir isotherm constant (L $mg^{-1}$). Values of the constants $q_{max}$ and $K_L$ were deduced from the slope and intercept of the linear plot of $\frac{C_e}{q_e}$ against $C_e$, respectively.

An important dimensionless index of Langmuir isotherm parameters, called the separation factor, $R_L$, is used to predict the efficiency of the adsorption process. Adsorption is considered unfavorable when $R_L > 1$; favorable when $0 < R_L < 1$; while $R_L = 1$ indicates linearity. The value of $R_L$ is defined by Equation (8):

$$R_L = \frac{1}{1 + (1 + K_L + C_o)} \tag{8}$$

where $C_o$ represents the initial concentration (mg $L^{-1}$) of adsorbates in solution.

Using the Langmuir isotherm, the maximum sorption capacities for monolayer coverage, $q_{max}$, in the removal of AMX, AMP, and CHLR from aqueous solutions with GSA and GSB were 2.28, 1.87, and 1.71 mg $g^{-1}$, respectively, and 1.51, 1.32, and 2.55 mg $g^{-1}$, respectively (Table 4). The separation factor $R_L$ for the sorption of the three antibiotics onto GSA and GSB were in the range of 0.19–0.87 and 0.14–0.91, respectively, which indicates favorable sorption with both adsorbents. The adsorption data fitted well to the Langmuir isotherm model giving high correlation coefficient values ($R^2 > 0.95$) with insignificant differences in their $R^2$-values ($\rho < 0.02$) (**Table 6**).

**Table 6.** Isotherms constants for the adsorption of antibiotics onto GSA and GSB.

| | AMX | | AMP | | CHLR | |
|---|---|---|---|---|---|---|
| Equilibrium model | GSA | GSB | GSA | GSB | GSA | GSB |
| Freundlich | | | | | | |
| $k_F$ ($mg\,g^{-1}$ [$L\,mg^{-1}$] 1/n) | 0.19 | 0.19 | 0.21 | 0.17 | 0.22 | 0.19 |
| $n_F$ | 0.99 | 0.99 | 0.87 | 0.90 | 0.65 | 0.97 |
| $R^2$ | 0.9946 | 0.9865 | 0.9869 | 0.9885 | 0.9763 | 0.9769 |
| Langmuir | | | | | | |
| $k_L$ ($L\,mg^{-1}$) | 0.001 | 0.004 | 0.06 | 0.014 | 0.04 | 0.02 |
| $q_{max}$ ($mg\,g^{-1}$) | 2.28 | 1.51 | 1.87 | 1.32 | 1.71 | 2.55 |
| $R_L$ | 0.33–0.61 | 0.14–0.67 | 0.25–0.87 | 0.75–0.91 | 0.19–0.44 | 0.32–0.61 |
| $R^2$ | 0.9905 | 0.9987 | 0.9896 | 0.9824 | 0.9585 | 0.9779 |

The Freundlich isotherm model which uses an empirical equation to describe a multilayer adsorption process was tested for the sorption of AMX, AMP and CHLR onto the activated carbons GSA and GSB. However, the Freundlich isotherm model is only valid where adsorption occurs on heterogenous surface.[27,67]

The linear form of the Freundlich model is expressed as

$$\ln q_e = \ln k_F + \frac{1}{n_F} \ln C_e \quad (9)$$

$k_F$ represents the Freundlich isotherm constant which relates to the adsorption capacity of the adsorbents; $n_F$ relates to the intensity of adsorption; $C_e$ is the equilibrium concentration of adsorbate at equilibrium ($mg\,L^{-1}$); and $q_e$ is the amount of adsorbate adsorbed per gram of the adsorbent at equilibrium ($mg\,g^{-1}$). The terms $k_F$ and $\frac{1}{n_F}$ are constants obtained from the slope and intercept of the plot of $\ln q_e$ versus $\ln C_e$, for the adsorption of the antibiotics onto GSA and GSB.

The term $n_F$ in the Freundlich isotherm measures the deviation of adsorption process from linearity. According to Pezoti et al.,[4] when $n_F = 1$ the adsorption process is linear; for $n_F < 1$ the adsorption process is essentially chemical and for $n_F > 1$ the adsorption process is essentially physical. Since the Freundlich isotherm term $n_F$ for the adsorption of AMX, AMP, and CHLR onto the activated carbons was <1 (calculated values of $n_F$ were <1), with high correlation coefficients ($R^2 > 0.97$) (Table 4), the adsorption processes are multi-layered and probably occurred largely on heterogenous adsorbents' surfaces. Yang et al.[68] and Pezoti et al.[4] suggested that when the sorption of adsorbates onto adsorbents are multi-layered, the adsorption process is influenced by chemical reactions that probably arose from the interactions of the adsorbate molecules with some functional groups on the adsorbents' surfaces.

The Temkin isotherm model mainly attempts to describe electrostatic interactions in chemical adsorption processes and its associated heat of adsorption.[69,70] Hence, the isotherm model describes adsorption parameters that indicate the possible existence of adsorbent–adsorbate interactions, with less emphasis on extremely low or large concentrations of the adsorbates.[41,70] The Temkin model also assumes a possibility for a linear decrease in the heat of adsorption process as the adsorbent surface gets saturated.

The linearized form of Temkin equation is as represented in Equation (10)

$$q_e = B\ \ln K_{TEM} + B\ \ln C_e \quad (10)$$

A plot of $q_e$ against $\ln C_e$ provides a linear regression from which the adsorption constant $K_{TEM}$ is determined (slope) while the intercept was used to derive $b_T$.[60,71]

The term $K_{TEM}$ is the Temkin isotherm equilibrium binding constant ($L\,g^{-1}$), $B$ is a constant related to the heat of adsorption ($J\,mol^{-1}$), $b_T$ is the Temkin isotherm constant showing variation of the adsorption energy ($kJ\,mol^{-1}$), $R$ is the universal gas constant ($8.314\,kJ\,mol^{-1}$), $T$ is the temperature (K), $C_e$ is the equilibrium concentration ($mg\,L^{-1}$), and $q_e$ is the amount of adsorbate adsorbed per gram of the adsorbent at equilibrium ($mg\,g^{-1}$).[71]

The $K_{TEM}$ values for the adsorption of AMX, AMP, and CHLR onto GSA and GSB were 1.168, 1.643, and $0.983\,L\,g^{-1}$, respectively, and 0.621, 0.660, and $0.850\,L\,g^{-1}$ for AMX, AMP, and CHLR, respectively. In addition, the Temkin isotherm constant ($B$) values for the adsorbate sorption onto GSA and GSB were 42.695, 41.515, and $52.710\,J\,mol^{-1}$, respectively, and 48.966, 45.903, and $64.797\,J\,mol^{-1}$, respectively. The correlation coefficient ($R^2$) values showed that data fitted well to the Temkin isotherm model. According to Rahardjo et al.,[72] experimental data fitting well to the Temkin isotherm model implies that the heat of adsorption associated with the sorption, decreases as the adsorbent surface coverage is enhanced.

As the data generated for the sorption processes of the antibiotics AMX, AMP, and CHLR onto GSA and GSB fit well to the three isotherm models tested, it is assumed that adsorption proceeded via a combination of chemisorption and physisorption onto heterogeneous surfaces, attaining saturation at some point as indicated by the Freundlich model. There is also an indication of adsorption onto monolayer surfaces with a finite number of adsorption sites, as shown by values obtained from the Langmuir isotherm model.

### *3.6.5. Effect of Temperature and Thermodynamics*

The equilibrium constant, $K_c$, and the standard Gibbs free energy change, $\Delta G^\circ$ ($kJ\,mol^{-1}$) for the adsorption process was

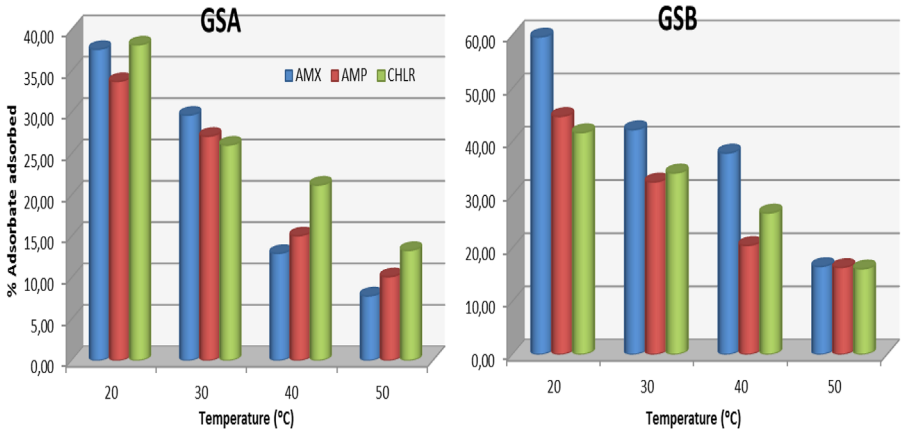


**Figure 8.** Percentage adsorbate adsorbed by GSA and GSB at various temperatures. Experimental conditions: concentration of adsorbate = 30 mg $L^{-1}$; volume of adsorbate solution = 25 mL; mass of adsorbent = 0.1 g; stirring speed = 120 rpm.

calculated using Equation (11) and (12), respectively, while the values of the standard enthalpy change, $\Delta H^{\circ}$ (kJ $mol^{-1}$), and standard entropy change, $\Delta S^{\circ}$ (J $K^{-1}$ $mol^{-1}$) were calculated from the intercept and the slope of the linear plot of ln $K_c$ versus $1/T$ (Equation (13)).

$$K_c = \frac{C_a}{C_e} \tag{11}$$

$$\Delta G^{\circ} = -RT \ln K_c \tag{12}$$

$$\ln K_c = \frac{\Delta S}{R} - \frac{\Delta H}{RT} \tag{13}$$

where $C_a$ is the amount of adsorbate removed by the adsorbent (mg $L^{-1}$) at equilibrium, $C_e$ is the equilibrium concentration (mg $L^{-1}$) of adsorbate, $R$ is the universal gas constant (8.314 J $K^{-1}$ $mol^{-1}$), $T$ is the absolute temperature ($K$), and $K_c$ is the thermodynamic equilibrium constant.

The adsorption data obtained for the sorption of AMX, AMP, and CHLR onto GSA and GSB at temperature ranging between 20 and 50 °C revealed a decrease in the adsorption capacity of the adsorbents with increases in solution temperature (**Figure 8**).

Changes in temperature appeared to induce an influence on the affinity between antibiotics and adsorbent surfaces. An increase in solution temperature imposes a negative affinity effect between the antibiotics and the adsorbents, thus, the reduction in the adsorbent sorption capacity. Munagapati and Kim[71] and Bansal[73] reported that sorption processes characterized by decrease in the adsorption of adsorbates onto an adsorbent with increasing temperature, is peculiar to exothermic adsorption processes. The decrease may be attributed to the weakening of the van der Waals forces of attraction between the antibiotic molecules and the adsorbents' surfaces.[74]

The adsorption enthalpy ($\Delta H^{\circ}$) values for the sorption of AMX, AMP, and CHLR onto both adsorbents were all negative (**Figure 9**). The net negative adsorption enthalpy, $\Delta H^{\circ}$, indicates that the molecular diffusion and repulsion between adsorbed molecules and desorption of solvent during the adsorption process was exothermic, with an affinitive binding of adsorbate

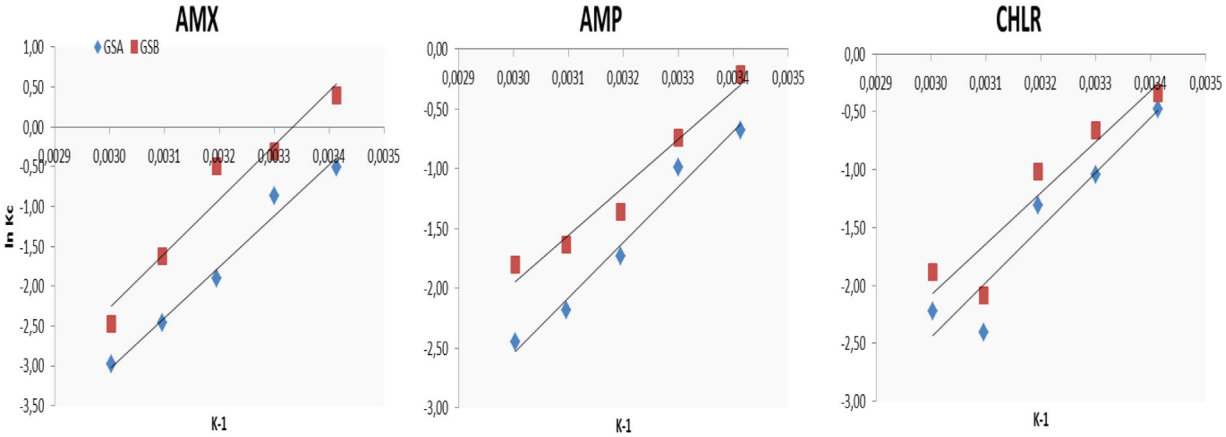


**Figure 9.** Van't Hoff plots for the adsorption of the adsorbates onto GSA and GSB.

molecules onto the adsorbent surface. This is indicative of chemisorption and consistent with the observed pseudo-second order kinetics of the sorption processes. Fan et al.[70] made similar observation at high $\Delta H^{\circ}$ values (>40 kJ $mol^{-1}$).

The entropy change ($\Delta S^{\circ}$) values were negative for the three antibiotics adsorbates on GSA and GSB. This implies that the entropy of the adsorbate molecules decreased with temperature increase, leading to a decrease in the randomness at the solid–solution interface during the sorption of the antibiotics onto the adsorbent surfaces. Reduction in entropy leads to a decrease in spontaneity at the adsorbent–solution interface during the sorption process.[75] Reactions such as association, fixation, or immobilization of adsorbate molecules due to adsorption, result in loss of degrees of freedom of adsorbate molecules, thereby producing negative entropy effects.

Generally, the sorption of the tested antibiotics onto the ACs prepared from grape slurry waste is a rapid process attaining equilibrium between 90 and 150 min. The distribution between the solid adsorbent and the liquid phase adsorbate is a function of the degree of the affinity of the adsorbent for the adsorbate, while the quality of the sorbent materials which is often judge based on the amount of the sorbate that can be attracted and retained in an immobilized form, appeared to be good since all adsorbents showed reasonably good antibiotic removal.

## 4. Conclusion

Three antibiotics studied, AMX, AMP, and CHLR, were detected in environmental water samples. Attempts were made to remediate these compounds using ACs produced from grape slurry waste. The antibiotics' removal efficiency was in the order GSB > GSA. The sorption data indicate that all the operating conditions employed in this study are crucial for the control of antibiotics adsorption. The percentage sorption was enhanced with increasing adsorbent dose, contact time, and pH, while increasing initial antibiotic concentration and temperature does not favor the sorption of the antibiotics. The equilibrium data fit satisfactorily to both Langmuir and Freundlich isotherms. In addition, the pseudo-second-order better described the adsorption of the antibiotics onto activated carbon from grape slurry waste. Thermodynamic evaluations also showed that the sorption process of AMX, AMP, and CHLR was exothermic, feasible but non-spontaneous in nature with increases in temperature. The findings of this study are very important and useful giving the potential and possibility of the adsorbents to be extended in remediation studies of other organic pollutants in wastewater.

## Abbreviations

AC, activated carbon; AMP, ampicillin; AMX, amoxicillin; CHLR, chloramphenicol; DAD, diode array detector; EDC, endocrine disrupting compound; EDX, energy dispersive X-ray; FTIR, Fourier transform infrared; GS, grape slurry; GSA, acid activated carbon prepared from grape slurry; GSB, base activated carbon prepared from grape slurry; HLB, hydrophilic/lipophilic balance; LOD, limit of detection; LOQ, limit of quantification; RSD, relative standard deviation; SEM, scanning electron microscopy; SPE, solid phase extraction; UHPLC, ultra-high performance liquid chromatography; UV, ultraviolet; WWTP, wastewater treatment plant.

## Conflict of Interest

The authors have declared no conflict of interest.

## Keywords

adsorption, antibiotics, biomass, remediation, wastewater treatment

Received: February 3, 2018
Revised: August 14, 2018
Published online: December 17, 2018

[1] J. E. Renew, C-H. Huang, *J. Chromatogr. A* **2004**, *1042*, 113.
[2] S. Manzetti, R. Ghisi, *Mar. Pollut. Bull* **2014**, *79*, 7.
[3] Q.-Q. Zhang, G.-G. Ying, C.-G. Pan, Y.-S. Liu, J.-L. Zhao, *Environ. Sci. Technol*. **2015**, *49*, 6772.
[4] O. Pezoti, A. L. Cazetta, K. C. Bedin, L. S. Souza, A. C. Martins, T. L. Silva, O. O. Santos, Jr., J. V. Visentainer, V. C. Almeida, *Chem. Eng. J*. **2016**, *288*, 778.
[5] L. M. Madikizela, N. T. Tavengwa, L. Chimuka, *J. Environ. Manage*. **2017**, *193*, 211.
[6] A. Jelic, M. Gros, A. Ginebreda, R. Cespedes-Sánchez, F. Ventura, M. Petrovic, D. Barcelo, *Water Res*. **2011**, *45*, 1165.
[7] V. Homem, L. Santos, *J. Environ. Manage*. **2011**, *92*, 2304.
[8] A. K. Sarmah, M. T. Meyer, A. B. Boxall, *Chemosphere* **2006**, *65*, 725.
[9] V. Rakic, N. Rajic, A. Dakovic, A. Auroux, *Microporous Mesoporous Mater.* **2013**, *166*, 185.
[10] S. K. Khetan, T. J. Collins, *Chem. Rev.* **2007**, *107*, 2319.
[11] V. Fessard, L. Le Hegarat, *Anal. Bioanal. Chem*. **2010**, *397*, 1715.
[12] J. Neuwoehner, B. I. Escher, *Aquat. Toxicol*. **2011**, *101*, 266.
[13] J. Martín, D. Camacho-Munoz, J. L. Santos, I. Aparicio, E. Alonso, *J. Hazard. Mater.* **2012**, *239-240*, 40.
[14] K. O. K'oreje, L. Vergeynst, D. Ombaka, P. De Wispelaere, M. Okoth, H. Van Langenhove, K. Demeestere, *Chemosphere* **2016**, *149*, 238.
[15] M. A. Chayid, M. J. Ahmed, *J. Environ. Chem. Eng*. **2015**, *3*, 1592.
[16] A. B. A. Boxall, L. A. Fogg, P. A. Blackwell, P. Kay, E. J. Pemberton, A. Croxford, *Rev. Environ. Contam. Toxicol*. **2004**, *80*, 1.
[17] K. V. Thomas, M. J. Hilton, *Mar. Pollut. Bull*. **2004**, *49*, 436.
[18] X. Wei, S. C. Wu, X. P. Nie, A. Yediler, M. H. Wong, *J. Environ. Sci. Health B* **2009**, *44*, 461.
[19] J.-P. Lumaret, F. Errouissi, K. Floate, J. Römbke, K. Wardhaugh, *Curr. Pharm. Biotechnol*. **2012**, *13*, 1004.
[20] L. Rizzo, C. Manaia, C. Merlin, T. Schwartz, C. Dagot, M. C. Ploy, I. Michael, D. Fatta-Kassinos, *Sci. Total Environ* **2013**, *447*, 345.
[21] M. Klavairoti, D. Mantzavinos, D. Kassinos, *Environ. Int.* **2009**, *35*, 402.
[22] P. Paiga, L. H. M. L. M. Santos, S. Ramos, S. Jorge, J. Gabriel Silva, C. Delerue-Matos, *Sci. Total Environ*. **2016**, *573*, 164.
[23] P. A Segura, H. Takada, J. A. Correa, K. El Saadi, T. Koike, S. Onwona-Agyeman, J. Ofosu-Anim, E. B. Sabi, O. V. Wasonga, J. M. Mghalu, A. M. dos Santos Junior, B. Newman, S. Weerts, V. Yargeau, *Environ. Int* **2015**, *80*, 89.
[24] R. Gurke, M. Robler, C. Marx, S. Diamond, S. Schubert, R. Oertel, J. Fauler, *Sci. Total Environ*. **2015**, *532*, 762.
[25] R. Moreno-Gonzalez, S. Rodriguez-Mozaz, M. Gros, D. Barcelo, V. M. Leon, *Environ. Res*. **2015**, *138*, 326.
[26] A. M. P. T. Pereira, L. J. G. Silva, L. M. Meisel, C. M. Lino, A. Pena, *Environ. Res*. **2015**, *136*, 108.

 

[27] A.Y. -c. Lin, T.-h. Yu, S. K. Lateef, *J. Hazard. Mater.* **2009**, *167*, 1163.
[28] M. Mehrjouei, S. Muller, D. Moller, *Chem. Eng. J.* **2014**, *248*, 184.
[29] M. R. Samarghandi, T. J. Al-Musawi, A. Mohseni-Bandpi, M. Zarrabi, *J. Mol. Liq.* **2015**, *211*, 431.
[30] S. Budyanto, S. Soedjono, W. Irawaty, N. Indraswati, *J. Environ. Prot. Sci.* **2008**, *2*, 72.
[31] S. Álvarez-Torrellas, R. García-Lovera, A. Rodríguez, J. Garcíaa, *Chem. Eng. Trans.* **2015**, *43*, 1963.
[32] C. Tan, Z. Zeyu, H. Rong, M. Ruihong, W. Hongtao, L. Wenjing, *Chemosphere* **2015**, *134*, **286**.
[33] G. Moussavi, A. Alahabadi, K. Yaghmaeian, M. Eskandari, *Chem. Eng. J.* **2013**, *217*, 119.
[34] N. Le-Minh, R. M. Stuetz, S. J. Khan, *Talanta* **2012**, *89*, 407.
[35] A. E. B. Kermia, D. Fouial-Djebbar, M. Trari, *C. R. Chim.* **2016**, *19*, 963.
[36] S. S. Zunngu, L. M. Madikizela, L. Chimuka, P. S. Mdluli, *C. R. Chim.* **2017**, *20*, 585.
[37] A. Nikolaou, S. Meric, D. Fatta, *Anal. Bioanal. Chem.* **2007**, *387*, 1225.
[38] A. Gulkowska, H. W. Leung, M. K. So, S. Taniyasu, N. Yamashita, L. W. Y. Yeung, B. J. Richardson, A. P. Lei, J. P. Giesy, P. K. S. Lam, *Water Res.* **2008**, *42*, 395.
[39] C. H. Huang, D. L. Sedlak, *Environ. Toxicol. Chem.* **2001**, *20*, 133.
[40] M. Nie, Y. Yang, Z. Zhang, C. Yan, X. Wang, H. Li, W. Dong, *Chem. Eng. J.* **2014**, *246*, 373.
[41] B. O. Fagbayigbo, B. O. Opeolu, O. S. Fatoki, O. S. Olatunji, *Environ. Sci. Pollut. Res.* **2017**, *24*, 1.
[42] F. Xu, Z. Tang, S. Huang, L. Chen, Y. Liang, W. Mai, H. Zhong, R. Fu, D. Wu, *Nat. Commun.* **2015**, *6*, 7221.
[43] M. Kosmulski, C. Saneluta, *J. Colloid Interface Sci.* **2004**, *280*, 544.
[44] M. Bedin, A. Karim, M. Reitti, A-C.C. Carlsson, F. Topic, M. Cetina, F. Pan, V. Havel, F. Al-Ameri, V. Sindelar, K. Rissanen, J. Gräfenstein, M. Erdelyi, *Chem. Sci.* **2015**, *6*, 3746.
[45] O. A. Ekpete, A. C. Marcus, V. Osi, *J. Chem.* **2017**, *8635615*, 1.
[46] O. S. Ayanda, O. Adeyi, B. Durojaiye, O. Olafisoye, *Pol. J. Environ. Stud.* **2012**, *21*, 1147.
[47] O. S. Fatoki, O. S. Ayanda, F. A. Adekola, B. J. Ximba, B. O. Opeolu, *Part. Part Syst. Char.* **2012**, *29*, 178.
[48] O. A. Ekpete, M. J. N. R. Horsfall, *Res. J. Chem. Sci.* **2011**, *1*, 10.
[49] A. H. Abdullah, A. Kassim, Z. Zainal, M. Z. Hussien, D. Kuang, F. Ahmad, O. S. Wooi, *Malaysian J. Anal. Sci.* **2001**, *7*, 65.
[50] P. Bartczak, M. Norman, L. Klapiszewski, N. Karwanska, M. Kawalee, M. Bacyynska, M. Wysokowski, J. Zdarta, F. Ciesielezyk, T. Jesionowski, *Arabian J. Chem.* **2015**, *30*, 456.
[51] Q. Zhang, K. T. Chuang, *Adv. Environ. Res.* **2001**, *5*, 251.
[52] Y. Roggo, P. Chalus, L. Maurer, C. Lema-Martinez, A. Edmond, N. Jent, *J. Pharm. Biomed. Anal.* **2007**, *44*, 683.
[53] W. Mozgawa, M. Krol, T. Bajda, *J. Mol. Struct.* **2011**, *993*, 109.
[54] M. Xie, L. D. Nghiem, W. E. Price, M. Elimelech, *Water Res.* **2012**, *46*, 2683.
[55] K. Ojha, N. C. Pradhan, A. N. Samanta, *Indian Acad. Sci.* **2004**, *27*, 555.
[56] D. Karami, S. Rohani, *Industr. Eng. Chem. Res.* **2009**, *48*, 4837.
[57] M. Gougazeh, J. C. Buhl, *J. Assoc. Arabian Univ. Basic Appl. Sci.* **2014**, *15*, 35.
[58] B. Zhang, H. Zhang, X. Li, X. Lei, C. Li, D. Yin, X Fan, Q. Zhang, *Mater. Sci. Eng.* **2013**, *33*, 4401.
[59] H. R. Pouretedal, N. Sadegh, *J. Water Process Eng.* **2014**, *1*, 64.
[60] B. H. Hameed, D. K. Mahmoud, A. L. Ahmad, *J. Hazard. Mater.* **2008**, *158*, 65.
[61] U. A. Guler, M. Sarioglu, *J. Environ. Health Sci. Eng.* **2014**, *12*, 1.
[62] S. E. Shaibu, F. A. Adekola, H. I. Adegoke, O. S. Ayanda, *Materials* **2014**, *7*, 4493.
[63] A. Kara, E. Demirbel, *Water Air Soil Pollut.* **2012**, *223*, 2387.
[64] R. Alfaro-Cuevas-Villanueva, A. R. Hidalgo-Vázquez, J. C. de Penagos, R. Cortés-Martínez, *Sci. World J.* **2014**, 647512.
[65] J. Zhang, Q. Zhou, L. Ou, *J. Chem. Eng. Data* **2012**, *57*, 412.
[66] H. Altaher, T. E. Khalil, R. Abubeah, *Colour. Technol.* **2014**, *130*, 205.
[67] S. X. Zha, Y. Zhou, X. Jin, Z. Chen, *J. Environ. Manage.* **2013**, *129*, 569.
[68] J. Yang, M. Yu, W. Chen, *J. Ind. Eng. Chem.* **2015**, *21*, 414.
[69] L. Leng, X. Yuan, H. Huang, J. Shao, H. Wang, X Chen, G. Zeng, *Appl. Surf. Sci.* **2015**, *346*, 223.
[70] S. Fan, Y. Wang, Z. Wang, J. Tang, J. Tang, X. Li, *J. Environ. Chem. Eng.* **2017**, *5*, 601.
[71] V. S. Munagapati, D. Kim, *Ecotoxicol. Environ. Saf.* **2017**, *141*, 226.
[72] A. K. Rahardjo, M. J. J. Susanto, A. Kurniawan, N. Indraswati, S. Ismadji, *J. Hazard. Mater.* **2011**, *190*, 1001.
[73] O. P. Bansal, *Natl. Acad. Sci. Lett.* **2012**, *35*, 109.
[74] S. Yang, J. Li, D. Shao, J. Hu, X. Wang, *J. Hazard. Mater.* **2009**, *166*, 109.
[75] E.-S. I. El-Shafey, H. Al-Lawati, A. S. Al-Sumri, *J. Environ. Sci* **2012**, *24*, 1579.